

### High spin states in <sup>99</sup>Tc

G. Kajrys, W. Del Bianco, S. Pilotte, S. Landsberger,\* and S. Monaro

*Laboratoire de Physique Nucléaire, Université de Montréal, Montréal, Québec, Canada H3C 3J7*

(Received 20 July 1984)

High spin states in <sup>99</sup>Tc have been populated via the <sup>96</sup>Zr(<sup>6</sup>Li,3n $\gamma$ ) reaction. In-beam  $\gamma$ - $\gamma$  coincidence techniques have been used to determine the level scheme while excitation function and angular distribution measurements have been used to assign spin values. The results are compared to previous work and the level systematics are discussed.

#### I. INTRODUCTION

In previous articles we reported on high and low spin states in <sup>97</sup>Tc populated via the <sup>94</sup>Zr(<sup>6</sup>Li,3n $\gamma$ ) (Ref. 1) and <sup>97</sup>Mo(p,n $\gamma$ ) (Refs. 2 and 3) reactions as part of a systematic study of the more neutron-rich transitional nuclei around mass 100. Current interest in this region is focused on the changes in nuclear structure that occur with increasing neutron number. Evidence for the onset of a stable deformation around  $N=60$  has been presented in a study on <sup>103</sup>Tc (Ref. 4), while a more gradual tendency towards deformation in the Rh nuclei is suggested by recent work on <sup>105-109</sup>Rh (Ref. 5). These light ion particle spectroscopy investigations, however, only provide information on low spin states, and little is presently known on high spin states in nuclei heavier than <sup>97</sup>Tc and <sup>103</sup>Rh. In this work we wish to present the results of a study of the high spin states in <sup>99</sup>Tc, populated via the <sup>96</sup>Zr(<sup>6</sup>Li,3n $\gamma$ ) reaction.

#### II. EXPERIMENTAL DETAILS

A 10 mg cm<sup>-2</sup> foil of enriched <sup>96</sup>Zr (85%) was bombarded with <sup>6</sup>Li ions from the Université de Montréal Tandem Accelerator. Singles  $\gamma$ -ray spectra up to 1.6 MeV in energy were taken at 20, 22, 23, 24, and 25 MeV bombarding energy with a Ge(Li) detector (resolution 2.0 keV at 1.33 MeV) placed 20 cm from the target at 90° to the beam direction. A typical spectrum, taken at 25 MeV bombarding energy, is shown in Fig. 1. The angular distributions of the deexcitation  $\gamma$  rays were measured between 0° and 90° to the beam direction in steps of 15° with the same detector placed 25 cm from the target. A NaI detector at -90° to the beam direction served as a normalization counter for each spectrum. A second Ge(Li) detector at -55° was added to obtain  $\gamma$ - $\gamma$  coincidence spectra. Standard electronics using constant fraction discrimination techniques were employed. Coincidences were recorded event by event onto magnetic tape and the prompt coincidence timing resolution achieved was  $\approx$ 15 ns. Coincidence spectra were generated by placing gates on the peaks observed in one detector and reconstructing the prompt coincidences observed in the second detector. Compton background and random time contributions were subtracted to obtain the final spectra, some examples of which are shown in Fig. 2.

For the angular distributions and excitation functions,  $\gamma$ -ray yields were determined using the peak fitting program SAMPO.<sup>6</sup> Once the decay scheme had been constructed from the coincidence data, possible spin estimates

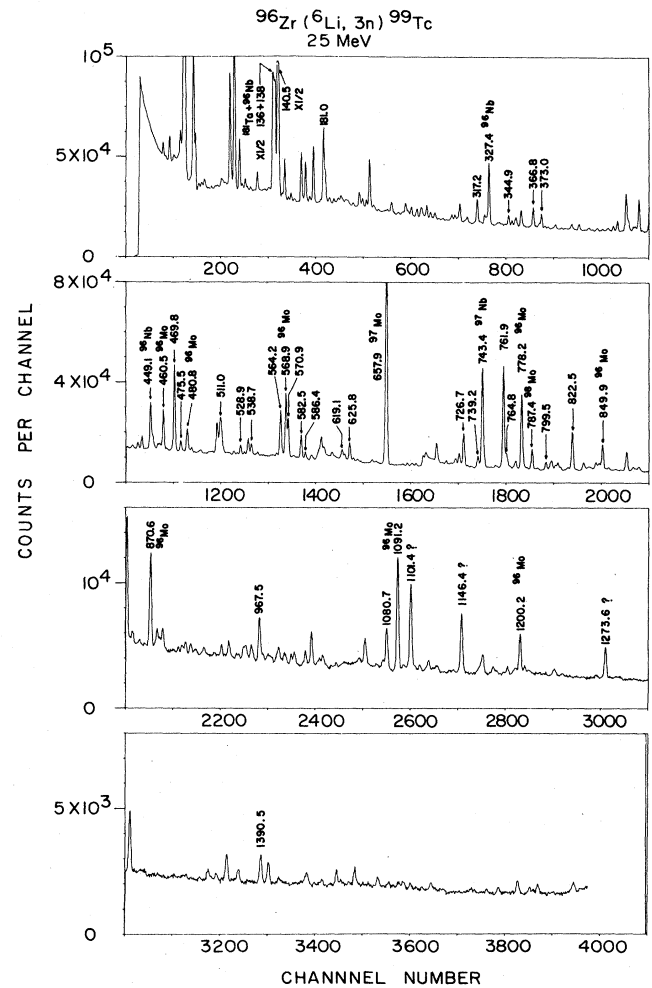


FIG. 1. A typical  $\gamma$ -ray spectrum observed in the <sup>96</sup>Zr(<sup>6</sup>Li,3n $\gamma$ ) reaction at 25 MeV bombarding energy. Energies are in keV and labeled peaks belong to <sup>99</sup>Tc unless otherwise specified.

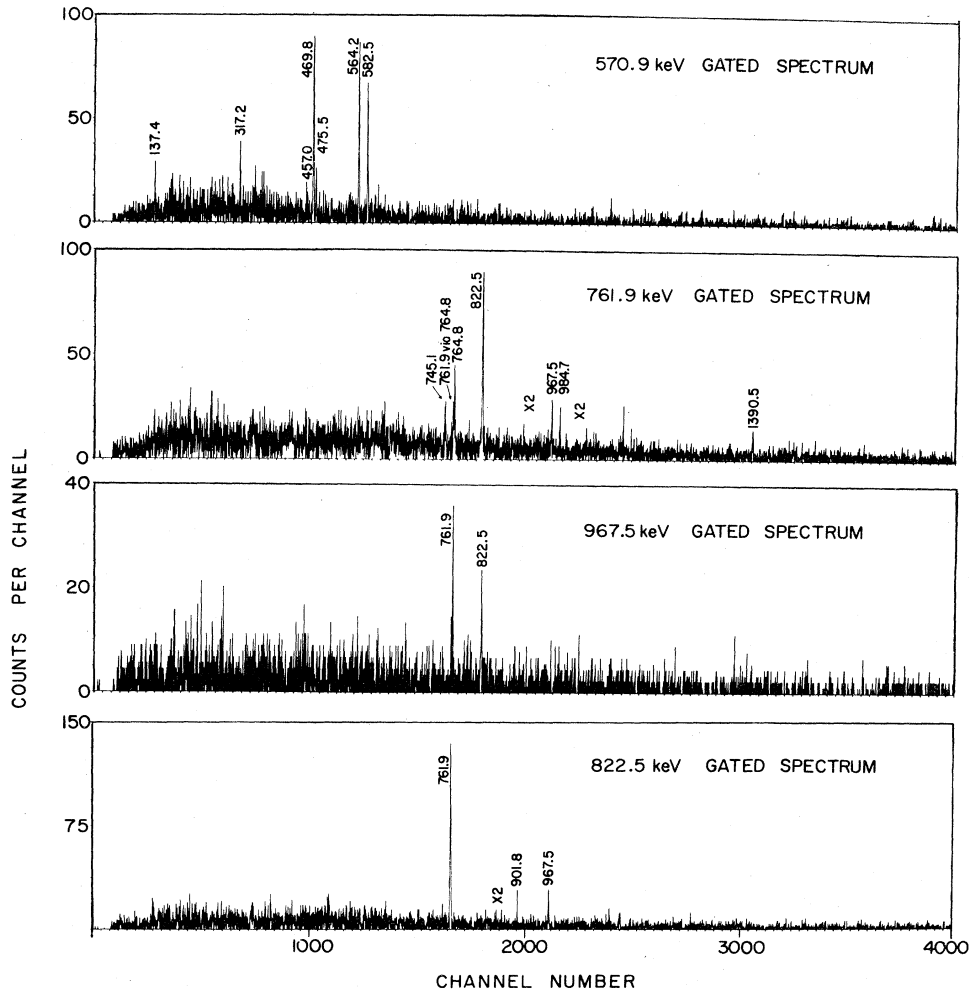


FIG. 2. Some examples of the  $\gamma$ - $\gamma$  coincidence data. Energies are in keV.

were obtained from the relative excitation functions, some of which are shown in Fig. 3. These possible spins were then used to fit the angular distribution data using techniques which are well documented<sup>7</sup> and will not be repeated here.

### III. RESULTS

The decay scheme of  $^{99}\text{Tc}$  as deduced in this work is shown in Fig. 4, while a summary of level energies,  $\gamma$ -ray energies, and angular distribution results is presented in Table I.

#### A. Low-lying levels

##### 1. The 0.0, 140.5, 142.6, and 181.0 keV levels

The ground state and first three excited states have spin-parities of  $\frac{9}{2}^+$ ,  $\frac{7}{2}^+$ ,  $\frac{1}{2}^-$ , and  $\frac{5}{2}^+$ , respectively, as deduced in  $^3\text{He,d}$  reaction work.<sup>9</sup> These assignments, for the positive parity levels, are also confirmed in Coulomb excitation work.<sup>10</sup> The 140.5 keV level is fed strongly by the decay of the  $\frac{1}{2}^-$ , 142.6 keV isomeric level and we are

not able to make any statement concerning the spins of these two levels from our work alone. The  $\frac{5}{2}^+$ , 181.0 keV level has a relatively long lifetime (3.6 ns) leading to an isotropic angular distribution. Our excitation function data, however, on the 181.0 keV transition do favor a  $\frac{5}{2}$  spin assignment (Fig. 3).

##### 2. The 509.4 and 534.3 keV levels

A strongly excited  $\frac{3}{2}^-$  state at 509 keV has been observed in ( $^3\text{He,d}$ ) reaction work<sup>9</sup> and in decay studies.<sup>11</sup> Our data on the possible 366.8 keV transition to the  $\frac{1}{2}^-$ , 142.6 keV state strongly support a  $\frac{3}{2}$  spin assignment. We have no evidence for the 534.3 keV level suggested by decay studies.<sup>11</sup>

#### B. Negative parity states above 509.4 keV

An intense 469.8 keV  $\gamma$  ray appears in the singles spectrum and is in strong coincidence with 564.2, 570.9, and 582.5 keV transitions, and we propose that it feeds the  $\frac{1}{2}^-$ , 142.6 keV state. The excitation function data on

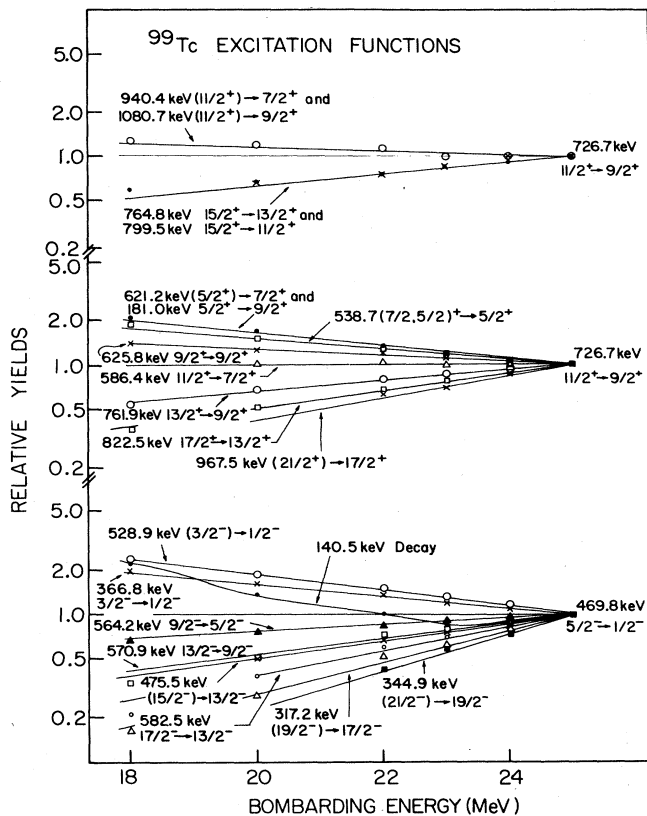


FIG. 3. Some relative excitation functions of  $\gamma$  rays belonging to  $^{99}\text{Tc}$ . Transitions involving negative parity states are normalized to the yield of the  $\frac{5}{2}^-$  to  $\frac{1}{2}^-$ , 469.8 keV  $\gamma$  ray. The yield of  $\gamma$  rays involving positive parity levels are normalized to the  $\frac{11}{2}^+$  to  $\frac{9}{2}^+$ , 726.7 keV  $\gamma$  ray.

these transitions (Fig. 3) show an increasing spin with increasing excitation energy, while the angular distribution data favor predominantly quadrupole transitions. We consequently assign spins and parities of  $\frac{5}{2}^-$ ,  $\frac{9}{2}^-$ ,  $\frac{13}{2}^-$ , and  $\frac{17}{2}^-$ , respectively, to the levels at 612.4, 1176.6, 1747.5, and 2330.0 keV. Three additional transitions feed this cascade forming levels at 2647.2, 2992.1, and 3129.5 keV. The angular distributions and excitation functions of the 317.2 and 344.9 keV transitions favor spins of  $\frac{19}{2}$  and  $\frac{21}{2}$ , respectively, for the levels at 2647.2 and 2992.1 keV. The 137.4 keV transition is a closely spaced doublet.

Three additional negative parity states are inferred from the  $\gamma$ - $\gamma$  coincidence data at 2223.0, 1604.5, and 985.4 keV. The 475.5-570.9-564.2-469.8 keV coincidences establish the level at 2223.0 keV. The excitation function and angular distribution data on the 475.5 keV transition favor a  $\frac{15}{2}^-$  spin-parity assignment.

The 469.8-373.0-619.1 keV coincidences establish the levels at 985.4 and 1604.5 keV. The excitation function of the 373.0 keV transition favors a spin of  $\frac{5}{2}$  while its angular distribution favors more a value of  $\frac{7}{2}$ . A possible 804.6 keV transition deexcites the 985.4 keV level to the  $\frac{5}{2}^+$ , 181.0 keV state, since 181.0 and 140.5 keV lines are seen weakly in the 804.6 keV gated spectrum. The 804.6

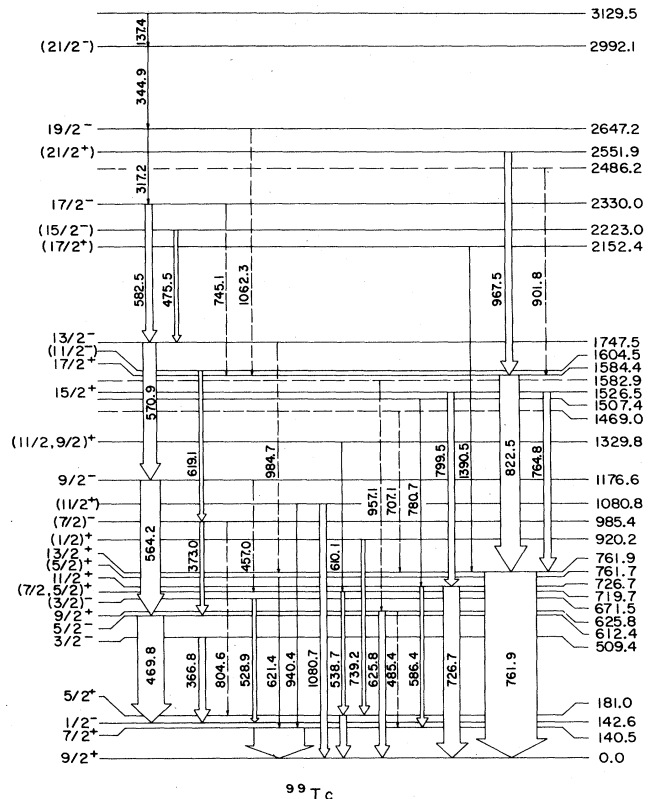


FIG. 4. The decay scheme of  $^{99}\text{Tc}$  as deduced in this work. Energies are in keV. Spins in parentheses are considered probable but not definitely established. Dotted levels and transitions are only weakly evident.

keV  $\gamma$  ray is a closely spaced doublet. The excitation function of the 619.1 keV transition favors a spin of  $\frac{11}{2}$  while its angular distribution has the shape of a predominantly quadrupole transition. An  $\frac{11}{2}^+$  spin-parity is probable for the 1604.5 keV level.

### C. Positive parity states above 509.4 keV

#### 1. The 625.8 and 671.5 keV levels

The level at 625.8 keV has been seen in  $^3\text{He,d}$  reaction and Coulomb excitation works<sup>9,10</sup> and a  $\frac{7}{2}^+$  or  $\frac{9}{2}^+$  spin-parity was assigned. The excitation function of the 625.8 keV ground state transition observed in our singles spectrum favors a  $\frac{9}{2}$  spin assignment, which is consistent with the angular distribution data. The 485.4 keV transition to the 140.5 keV,  $\frac{7}{2}^+$  state<sup>10</sup> was seen only weakly here and is left dotted in the decay scheme.

A  $\frac{5}{2}^+$  spin-parity was assigned to the weakly excited 672 keV level in  $^3\text{He,d}$  reaction work.<sup>9</sup> Our data on the 528.9 keV transition strongly favor a  $\frac{3}{2}$  spin assignment.

#### 2. The 719.7, 726.7, and 761.7 keV levels

The level at 719.7 keV is inferred by the 538.7-181.0 keV coincidence. The excitation function of the 538.7

TABLE I. A summary of level energies,  $\gamma$ -ray energies, relative intensities, and angular distribution results obtained for  $^{99}\text{Tc}$  in this work.

Level energy (keV)	$\gamma$ -ray energy (keV)	Relative intensity (%)	$J_i^\pi \rightarrow J_f^\pi$	$A_2$	$A_4$	$\delta^a$
140.5	140.5	106.5 $\pm$ 2.0	$\frac{7}{2}^+ \rightarrow \frac{9}{2}^+$	-0.06 $\pm$ 0.03	-0.01 $\pm$ 0.04	
142.6	$t_{1/2}=6.02$ h		$\frac{1}{2}^-$			
181.0	181.0	14.8 $\pm$ 0.3	$\frac{5}{2}^+ \rightarrow \frac{9}{2}^+$	-0.02 $\pm$ 0.03	-0.02 $\pm$ 0.04	
509.4	366.8	7.3 $\pm$ 0.2	$\frac{3}{2}^- \rightarrow \frac{1}{2}^-$	-0.18 $\pm$ 0.02	0.01 $\pm$ 0.02	
612.4	469.8	46.3 $\pm$ 1.0	$\frac{5}{2}^- \rightarrow \frac{1}{2}^-$	0.15 $\pm$ 0.04	-0.06 $\pm$ 0.05	
625.8	485.4 <sup>b</sup>	<2	$\frac{9}{2}^+ \rightarrow \frac{7}{2}^+$			
	625.8	12.8 $\pm$ 0.4	$\rightarrow \frac{9}{2}^+$	0.10 $\pm$ 0.03	-0.02 $\pm$ 0.04	
671.5	528.9	5.0 $\pm$ 0.2	$(\frac{3}{2}^\pm) \rightarrow \frac{1}{2}^-$	-0.09 $\pm$ 0.02	-0.00 $\pm$ 0.03	
719.7	538.7	6.4 $\pm$ 0.2	$(\frac{7}{2}, \frac{5}{2})^+ \rightarrow \frac{5}{2}^+$	-0.09 $\pm$ 0.04	-0.01 $\pm$ 0.05 ←	
726.7	726.7	31.4 $\pm$ 0.5	$\frac{11}{2}^+ \rightarrow \frac{9}{2}^+$	0.36 $\pm$ 0.02	0.01 $\pm$ 0.03	-0.9 $\pm$ 0.2
	586.4	4.8 $\pm$ 0.2	$\rightarrow \frac{7}{2}^+$	0.15 $\pm$ 0.04	-0.09 $\pm$ 0.04	E2
761.7	621.2	2.7 $\pm$ 0.2	$(\frac{5}{2}^+) \rightarrow \frac{7}{2}^+$	-0.11 $\pm$ 0.03	-0.05 $\pm$ 0.04	
761.9	761.9	100	$\frac{13}{2}^+ \rightarrow \frac{9}{2}^+$	0.20 $\pm$ 0.03	-0.06 $\pm$ 0.03	E2
920.2	739.2	8.8 $\pm$ 0.4	$(\frac{1}{2}^+) \rightarrow \frac{5}{2}^+$	-0.00 $\pm$ 0.02	-0.02 $\pm$ 0.03	
985.4	373.0	5.0 $\pm$ 0.1	$(\frac{7}{2}^-) \rightarrow \frac{5}{2}^-$	-0.33 $\pm$ 0.03	0.06 $\pm$ 0.04	+2.5 $^{+0.5}_{-0.4}$
	804.6 <sup>c</sup>	5.5 $\pm$ 0.2	$\rightarrow \frac{5}{2}^+$	-0.17 $\pm$ 0.02	0.01 $\pm$ 0.03	E2
1080.8	940.4	3.7 $\pm$ 0.2	$(\frac{11}{2}^+) \rightarrow \frac{7}{2}^+$	0.18 $\pm$ 0.03	-0.05 $\pm$ 0.04	E2
	1080.7	7.5 $\pm$ 0.4	$\rightarrow \frac{9}{2}^+$	-0.42 $\pm$ 0.03	0.02 $\pm$ 0.03	
1176.6	564.2	31.1 $\pm$ 1.0	$\frac{9}{2}^- \rightarrow \frac{5}{2}^-$	0.17 $\pm$ 0.04	-0.07 $\pm$ 0.05	E2

TABLE I. (Continued).

Level energy (keV)	$\gamma$ -ray energy (keV)	Relative intensity (%)	$J_i^\pi \rightarrow J_f^\pi$	$A_2$	$A_4$	$\delta^a$
1329.8	610.1	$3.0 \pm 0.1$	$(\frac{11}{2}, \frac{9}{2}^+) \rightarrow (\frac{7}{2}, \frac{5}{2})^+$	0.15 $\pm 0.04$	-0.03 $\pm 0.05$	
1469.0	707.1 <sup>b</sup>	< 1	$\rightarrow \frac{13}{2}$			
1507.4	780.7	$2.7 \pm 0.1$	$\rightarrow \frac{11}{2}^+$	0.33 $\pm 0.04$	-0.14 $\pm 0.005$	
1526.5	764.8	$13.2 \pm 0.3$	$\frac{15}{2}^+ \rightarrow \frac{13}{2}^+$	0.25 $\pm 0.02$	-0.05 $\pm 0.03$	$0.7 \pm 0.2$
	799.5	$8.0 \pm 0.2$	$\rightarrow \frac{11}{2}^+$	0.19 $\pm 0.04$	-0.07 $\pm 0.04$	E2
1582.9	957.1 <sup>c</sup>		$\rightarrow \frac{9}{2}^+$			
1584.4	822.5	$41.7 \pm 1.0$	$\frac{17}{2}^+ \rightarrow \frac{13}{2}^+$	0.19 $\pm 0.02$	-0.08 $\pm 0.02$	E2
1604.5	619.1	$6.5 \pm 0.2$	$(\frac{11}{2}^-) \rightarrow (\frac{7}{2}^-)$	0.14 $\pm 0.03$	-0.10 $\pm 0.04$	E2
1745.7 $\leftarrow$	570.9	$25.8 \pm 0.6$	$\frac{13}{2}^- \rightarrow \frac{9}{2}^-$	0.19 $\pm 0.04$	-0.07 $\pm 0.05$	
	984.7	$3.7 \pm 0.2$	$\rightarrow \frac{13}{2}^+$	0.23 $\pm 0.04$	-0.02 $\pm 0.05$	
2152.4	1390.5	$6.4 \pm 0.2$	$(\frac{17}{2}^+) \rightarrow \frac{13}{2}^+$	0.29 $\pm 0.03$	-0.10 $\pm 0.03$	E2
2223.0	475.5	$5.0 \pm 0.1$	$(\frac{15}{2}^-) \rightarrow \frac{13}{2}^-$	-0.10 $\pm 0.03$	0.00 $\pm 0.03$	
2330.0	582.5	$17.7 \pm 0.5$	$\frac{17}{2}^- \rightarrow \frac{13}{2}^-$	0.23 $\pm 0.04$	-0.10 $\pm 0.05$	E2
	745.1		$\rightarrow \frac{17}{2}^+$			
2486.2	901.8	< 2	$\rightarrow \frac{17}{2}^+$			
2551.9	967.5	$11.0 \pm 0.3$	$(\frac{21}{2}^+) \rightarrow \frac{17}{2}^+$	0.14 $\pm 0.02$	-0.10 $\pm 0.03$	E2
2647.2	317.2	$7.4 \pm 0.2$	$\frac{19}{2}^- \rightarrow \frac{17}{2}^-$	-0.17 $\pm 0.02$	0.03 $\pm 0.02$	M1
	1062.3	$4.7 \pm 0.1$	$\rightarrow \frac{17}{2}^+$	-0.42 $\pm 0.03$	0.18 $\pm 0.04$	
2992.1	344.9	$3.5 \pm 0.2$	$(\frac{21}{2}^-) \rightarrow \frac{19}{2}^-$	-0.14 $\pm 0.02$	0.05 $\pm 0.03$	M1
3129.5	137.4 <sup>c</sup>	$39.4 \pm 1.0$	$\rightarrow \frac{21}{2}^-$	-0.16 $\pm 0.04$	0.02 $\pm 0.04$	

<sup>a</sup>E2/M1 mixing ratio. Sign convention of Rose and Brink (Ref. 8).<sup>b</sup>Weak transition.<sup>c</sup>Closely spaced doublet.

keV transition favors a  $\frac{7}{2}$  or  $\frac{5}{2}$  spin. Both values are consistent with the angular distribution data. This level was weakly excited in  $^3\text{He,d}$  reaction work<sup>9</sup> where a spin-parity of  $\frac{9}{2}^+$  or  $\frac{7}{2}^+$  was inferred. A possible weak 457.0 keV transition connects this level to the  $\frac{9}{2}^-$  state at 1176.6 keV. This transition is left dotted in the decay scheme.

The 726.7 keV level is well established in Coulomb excitation work<sup>10</sup> decaying via 726.7 and 586.4 keV transitions to the ground state and 140.5 keV state, respectively. Our data fully support the  $\frac{11}{2}^+$  spin-parity suggested in that work.

The  $\frac{5}{2}^+$  level at 761.7 keV was strongly excited in  $^3\text{He,d}$  reaction work<sup>9</sup> and in a Coulomb excitation study.<sup>10</sup> Only the 621.4 keV transition was observed in our work and our data support the  $\frac{5}{2}^+$  assignment.

### 3. The 761.9, 1526.5, 1584.4, and 2551.9 keV levels

The intense 761.9 keV  $\gamma$  ray in the singles spectrum confirms the  $\frac{13}{2}^+$  level at 762 keV observed in Coulomb excitation work<sup>10</sup> and our data add nothing new. Three transitions are seen strongly in coincidence with the 761.9 keV line at 764.8, 822.5, and 967.5 keV. The latter two transitions are in coincidence with each other so that new levels are formed at 1526.5, 1584.4, and 2551.9 keV. The 822.5 and 967.5 keV transitions have a predominantly quadrupole character while the excitation function data show an increasing spin, favoring  $\frac{17}{2}^+$  and  $\frac{21}{2}^+$  spin-parity assignments. Further support for the level at 1526.5 keV comes from the strong 726.7-799.5 keV coincidence. The 799.5 and 764.8 keV transitions have the same excitation function favoring a  $\frac{13}{2}$  or  $\frac{15}{2}$  spin assignment, with the latter clearly favored by the angular distribution data on both transitions.

The coincidence data suggest weak transitions connecting the level at 1747.5 keV ( $\frac{13}{2}^-$ ) with the 761.9 keV ( $\frac{13}{2}^+$ ) level and the levels at 2647.2 keV ( $\frac{19}{2}^-$ ) and 2330.0 keV ( $\frac{17}{2}^-$ ) with the 1584.4 keV level ( $\frac{17}{2}^+$ ).

### 4. The 920.2 and 1080.8 keV levels

A  $\frac{1}{2}^+$  level at 919 keV has been observed in  $^3\text{He,d}$  reaction work<sup>9</sup> and is strongly populated in the decay of  $^{99}\text{Mo}$  (Ref. 11) where a spin  $\frac{3}{2}^+$  is proposed. Since we cannot rule out the production of  $^{99}\text{Mo}$  in this work we can say little on the spin of this level.

A level at 1081.4 keV has been observed in Coulomb excitation work<sup>10</sup> with an  $\frac{11}{2}^+$  or  $\frac{9}{2}^+$  spin-parity assignment. In our work it is based on the 940.4-140.5 keV coincidence and the presence in the singles spectrum of the 1080.7 keV ground state transition. An  $\frac{11}{2}$  or  $\frac{9}{2}$  spin is suggested by the excitation function data with the former favored by the angular distribution of both transitions.

### 5. The 1329.8, 1469.0, 1507.4, and 1582.9 keV levels

The 610.1-538.7 keV coincidence establishes a new level at 1329.8 keV. An  $\frac{11}{2}^+$  or  $\frac{9}{2}^+$  spin-parity is consistent with the excitation function and angular distribution data

on the 610.1 keV transition.

The existence of the 1469.0 keV level is weakly suggested only on the basis of  $\gamma$ - $\gamma$  coincidence data and we can say little about it.

The level at 1507.4 keV is more firmly established via the 780.7-726.7 keV coincidences. The 780.7 keV  $\gamma$  ray lies on the edge of the intense 778.0 keV line and we can say little on the spin of the 1507.4 keV level.

The presence of a weak 957.1 keV line in the 625.8 keV gated spectrum suggests a level at 1582.9 keV. The 957.1 keV  $\gamma$  ray is a doublet and we can say little on the spin of this level.

### 6. The 2152.4 and 2486.2 keV levels

The level at 2152.4 keV is established from the 1390.5-761.9 keV coincidence with a spin of  $\frac{17}{2}$  or  $\frac{15}{2}$  suggested by the excitation function data. The predominantly quadrupole character of the 1390.5 keV transition strongly favors a  $\frac{17}{2}^+$  spin-parity assignment.

The 2486.2 keV level is only weakly established via the 761.9-822.5-901.8 keV coincidences. The weakness of the 901.8 keV transition precludes any further statement concerning this level.

## IV. DISCUSSION AND CONCLUSION

In Fig. 5 we compare the positive parity levels in  $^{95}\text{Tc}$  through  $^{103}\text{Tc}$ . We include the low lying  $\frac{5}{2}^+$  and  $\frac{7}{2}^+$  anomalous coupling states which are known for all these nuclei<sup>4,11</sup> and the one- and two-phonon coupled  $\frac{13}{2}^+$ ,  $\frac{11}{2}^+$ , and  $\frac{17}{2}^+$ ,  $\frac{15}{2}^+$  doublets which are now known in  $^{95}\text{Tc}$  through  $^{99}\text{Tc}$  (Refs. 1 and 11 and the present work). The  $\frac{13}{2}^+$  and  $\frac{17}{2}^+$  assignments in  $^{101}\text{Tc}$  are tentative,<sup>12</sup> while such states have not yet been observed in  $^{103}\text{Tc}$ . A second set of states ( $\frac{5}{2}^+$ ,  $\frac{7}{2}^+$ ,  $\frac{9}{2}^+$ ) which lie closest to the  $\frac{13}{2}^+$  state are also included in the figure for  $^{95}\text{Tc}$  through  $^{99}\text{Tc}$  (Refs. 1, 2, 11, and the present work). The positions of the  $2^+$  and  $4^+$  states in the corresponding  $A-1$  even-even Mo isotopes are indicated. The  $\frac{13}{2}^+$ ,  $\frac{11}{2}^+$  and  $\frac{17}{2}^+$ ,  $\frac{15}{2}^+$  states follow quite closely the positions of the  $2^+$  and  $4^+$  core states up to  $^{99}\text{Tc}$ . In  $^{101}\text{Tc}$  the  $\frac{13}{2}^+$  and  $\frac{17}{2}^+$  states lie well above the core states, a common feature in the neutron-rich Rh and Ag nuclei.<sup>11,13,14</sup> The

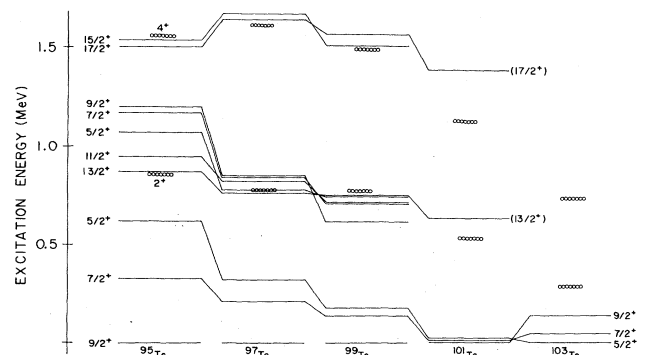


FIG. 5. A comparison of the positive parity levels in  $^{95}\text{Tc}$  through  $^{103}\text{Tc}$ .

anomalous coupling state show a rapid drop in energy with increasing mass, and the  $\frac{9}{2}^+$ ,  $\frac{7}{2}^+$ ,  $\frac{5}{2}^+$  level ordering in  $^{95}\text{Tc}$  is reversed in  $^{103}\text{Tc}$ . This change in structure coincides with the move to a stable quadrupole deformation by the underlying core.<sup>4</sup> The second  $\frac{9}{2}^+$  and  $\frac{7}{2}^+$  states also show a large drop in energy with increasing neutron number.

The Alaga model,<sup>15</sup> where a three proton cluster is coupled to a vibrational core, is not successful in describing the heavier Tc isotopes, although reasonable qualitative agreement is obtained for  $^{95}\text{Tc}$  and  $^{97}\text{Tc}$ . A slightly better fit is obtained when one considers a five proton cluster,<sup>16</sup> but again qualitative agreement is good only for the lighter nuclei.

The most successful calculations involve the interacting boson-fermion model<sup>17</sup> (IBFM) where a core of *s* and *d* bosons is coupled to an extra core particle. Detailed calculations have been reported only for  $^{97}\text{Tc}$  (Ref. 18) and  $^{103}\text{Tc}$  (Ref. 4). The agreement for  $^{97}\text{Tc}$  is excellent, even with a relatively simple, single *j* shell for the valence nucleons. Given the large change in structure in going from  $^{95}\text{Tc}$  to  $^{99}\text{Tc}$  it would be interesting to carry out detailed calculations also for  $^{95}\text{Tc}$  and  $^{99}\text{Tc}$ . More data are clearly needed on  $^{101}\text{Tc}$  so that the systematics of the model may be investigated.

Little work has yet been done on the Tc isotopes to calculate negative parity states in the framework of the IBFM. A summary of these states is shown in Fig. 6 for

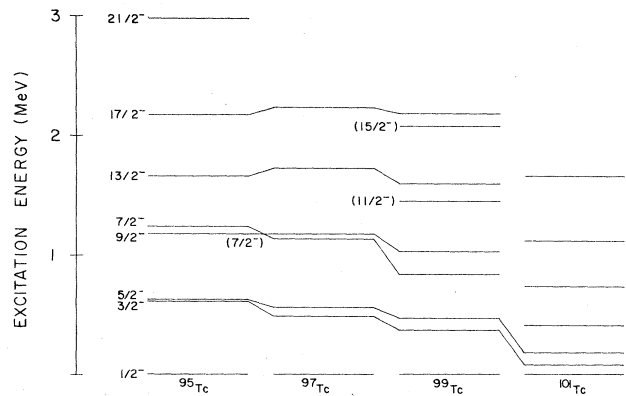


FIG. 6. A comparison of the band structure of negative parity levels in  $^{95}\text{Tc}$  through  $^{101}\text{Tc}$ .

$^{95}\text{Tc}$  through  $^{101}\text{Tc}$ . Unfortunately few spin assignments are available in  $^{101}\text{Tc}$ . Nevertheless, a large change in structure between  $^{97}\text{Tc}$  and  $^{101}\text{Tc}$  is apparent, reflecting a possible move to a permanently deformed shape. Similar band structures have been observed in  $^{99}\text{Rh}$ ,  $^{101}\text{Rh}$ , and  $^{103}\text{Rh}$  (Refs. 13 and 14) which seem to be well explained via the IBFM (Refs. 19 and 20). Enough data are now available for similar calculations in the odd-mass Tc nuclei to be performed.

\*Present address: Nuclear Activation Services Ltd., Nuclear Research Building, 1280 Main Street West, Hamilton, Ontario, Canada L8S 4K1.

<sup>1</sup>G. Kajrys, M. Irshad, S. Landsberger, R. Lecomte, P. Paradis, and S. Monaro, Phys. Rev. C **26**, 1462 (1982).

<sup>2</sup>S. Landsberger, R. Lecomte, P. Paradis, and S. Monaro, Nucl. Phys. A **339**, 238 (1980).

<sup>3</sup>G. Kajrys, S. Landsberger, R. Lecomte, P. Paradis, and S. Monaro, Phys. Rev. C **26**, 1451 (1982).

<sup>4</sup>P. De Gelder, D. De Frenne, K. Heyde, N. Kaffrell, A. M. Van den Berg, N. Blasi, M. N. Harakeh, and W. A. Sterrenburg, Nucl. Phys. A **401**, 397 (1983).

<sup>5</sup>E. R. Flynn, F. Ajzenberg-Selove, R. E. Brown, J. A. Cizewski, and J. W. Sunier, Phys. Rev. C **27**, 2587 (1983).

<sup>6</sup>J. T. Routti and S. G. Poussin, Nucl. Instrum. **72**, 125 (1969).

<sup>7</sup>P. Taras and B. Haas, Nucl. Instrum. Methods **123**, 73 (1975).

<sup>8</sup>H. J. Rose and D. M. Brink, Rev. Mod. Phys. **39**, 306 (1967).

<sup>9</sup>H. C. Cheung, S. I. Hayakawa, J. E. Kitching, J. K. P. Lee, S. K. Mark, and J. C. Waddington, Z. Phys. A **280**, 149 (1977).

<sup>10</sup>L. G. Svensson, D. G. Sarantites, and A. Bäcklin, Nucl. Phys.

A **267**, 190 (1976).

<sup>11</sup>Table of Isotopes, 7th ed., edited by C. M. Lederer and V. S. Shirley (Wiley, New York, 1978), p. 426 and references therein.

<sup>12</sup>D. R. Haenni, H. Dejbakhsh, R. P. Schmitt, and G. Mouchaty, Cyclotron Institute, Texas A&M University, Annual Report, 1983, Vol. 2.

<sup>13</sup>G. Kajrys, M. Irshad, S. Landsberger, R. Lecomte, P. Paradis, and S. Monaro, Phys. Rev. C **26**, 138 (1982).

<sup>14</sup>G. Kajrys, S. Landsberger, and S. Monaro, Phys. Rev. C **28**, 2335 (1983).

<sup>15</sup>S. M. Abecasis, O. Civitarese, and F. Krmpotic, Z. Phys. A **278**, 309 (1976).

<sup>16</sup>Chr. Bargholtz and S. Beshai, Z. Phys. A **283**, 89 (1977).

<sup>17</sup>F. Iachello and O. Scholten, Phys. Rev. Lett. **43**, 679 (1979).

<sup>18</sup>U. Kaup, R. Vorwerk, D. Hippe, H.-W. Schuh, P. von Brentano, and O. Scholten, Phys. Lett. **106B**, 439 (1981).

<sup>19</sup>G. Kajrys, S. Pilotte, G. Dufour, and S. Monaro, Phys. Rev. C **30**, 831 (1984).

<sup>20</sup>J. Vervier and R. V. F. Jansens, Phys. Lett. **B108**, 1 (1982).